

Discovery of extended X-ray emission around the highly magnetic RRAT J1819–1458

N. Rea¹, M. A. McLaughlin^{2,3,4}, B. M. Gaensler⁵, P. O. Slane⁶, L. Stella⁷,
S. P. Reynolds⁸, M. Burgay⁹, G. L. Israel⁷, A. Possenti⁹, S. Chatterjee¹⁰

ABSTRACT

We report on the discovery of extended X-ray emission around the high magnetic field Rotating Radio Transient J1819–1458. Using a 30 ks *Chandra* ACIS-S observation, we found significant evidence for extended X-ray emission with a peculiar shape: a compact region out to $\sim 5.5''$, and more diffuse emission extending out to $\sim 13''$ from the source. The most plausible interpretation is a nebula somehow powered by the pulsar, although the small number of counts prevents a conclusive answer on the nature of this emission. RRAT J1819–1458’s spin-down energy loss rate ($\dot{E}_{\text{rot}} \sim 3 \times 10^{32} \text{ erg s}^{-1}$) is much lower than that of other pulsars with observed spin-down powered pulsar wind nebulae (PWNe), and implies a rather high X-ray efficiency of $\eta_X \equiv L_{\text{pwn};0.5-8\text{keV}}/\dot{E}_{\text{rot}} \sim 0.2$ at converting spin-down power into the PWN X-ray emission. This suggests the need of an additional source of energy rather than the spin-down power alone, such as the high magnetic energy of this source. Furthermore, this *Chandra* observation allowed us to refine the positional accuracy of RRAT J1819–1458 to a

¹Astronomical Institute “Anton Pannekoek”, University of Amsterdam, Science Park 904, Postbus 94249, 1090 GE, Amsterdam, The Netherlands; n.rea@uva.nl

²Department of Physics, West Virginia University, Morgantown, WV 26501, USA

³National Radio Astronomy Observatory, Green Bank, WV 24944, USA

⁴Alfred P. Sloan Research Fellow

⁵Sydney Institute for Astronomy, School of Physics, The University of Sydney, NSW 2006, Australia

⁶Harvard-Smithsonian Center for Astrophysics, 60 Garden Street, Cambridge, MA 02138, USA

⁷INAF-Osservatorio Astronomico di Roma, via Frascati 33, I-00040 Monteporzio Catone, Italy

⁸Department of Physics, North Carolina State University, P.O. Box 8202, Raleigh, NC 27695, USA

⁹INAF-Osservatorio Astronomico di Cagliari, Loc. Poggio dei Pini, Strada 54, 09012 Capoterra, Italy

¹⁰Department of Astronomy and National Astronomy and Ionosphere Center, Cornell University, Ithaca, NY 14853-6801, USA

radius of $\sim 0.3''$, and confirms the presence of X-ray pulsations and the ~ 1 keV absorption line, previously observed in the X-ray emission of this source.

Subject headings: pulsar: individual (RRAT J1819–1458) — stars: magnetic fields — X-rays: stars

1. INTRODUCTION

All pulsars lose energy through a wind of relativistic particles. This relativistic wind has long been recognized to shock against the ambient medium, giving rise to “nebulae” powered by the pulsars, which usually emit at X-ray and radio wavelengths. It can be expected that all pulsars will be surrounded by such nebulae, usually powered by the pulsar rotational energy. The brightness and shapes of these nebulae depend on the pulsar properties, on the ambient medium density and anisotropies, and on the pulsar proper motion. In the most idealized case, an isotropic wind would form a spherical termination shock (Kennel & Coroniti 1984). The superb angular resolution of *Chandra* has resulted in the detection of roughly 50 nebulae, and has shown that this idealized description is not sufficient to describe most of their structures (Gaensler & Slane 2006; Kargaltsev & Pavlov 2008). In general, these nebulae are anisotropic, show equatorial and polar outflows, and have rich spectral structures. Most of the nebulae detected thus far are associated with pulsars with high spin-down energy loss rates ($\dot{E}_{\text{rot}} > 10^{33}$ ergs), the so called spin-down powered pulsar wind nebulae (PWNe), but there are a few cases where a nebula is observed but no pulsar is detected. The exact physical origin and acceleration mechanism of the high-energy particles in the pulsar winds are poorly understood, and not all nebulae can be easily explained as spin-down powered PWNe.

Rotating radio transients (RRATs) are peculiar neutron stars which, unlike normal radio pulsars, are detectable only through their sporadic radio bursts (McLaughlin et al. 2006). We currently know of over 20 of these objects (Deneva et al. 2008; Keane et al. 2009); they show a rather broad range of spin-down properties, with inferred surface dipole magnetic field strengths ranging from $2 \times 10^{12} - 5 \times 10^{13}$ G and characteristic ages ranging from 0.1–4 Myr. No sign of a companion star has yet been found for any of these objects.

RRAT J1819–1458 shows the most extreme and varied phenomenology of all the RRATs, and is the best studied object in the class. Radio bursts are detected every ~ 3 minutes, and two glitches have been observed which showed anomalous post-glitch recovery (Lyne et al. 2009). RRAT J1819–1458 has a 4.3 s spin period, a characteristic age of 117 kyr and a spin-down energy loss rate \dot{E}_{rot} of 3×10^{32} erg s $^{-1}$. The inferred surface dipolar magnetic field of

$B \sim 5 \times 10^{13}$ G is slightly higher than the electron critical magnetic field of $B_{\text{cr}} = 4.4 \times 10^{13}$ G, suggesting a possible relationship with magnetars. By using the dispersion measure and the Cordes & Lazio (2002) electron density model, the distance of RRAT J1819–1458 is estimated to be 3.6 kpc. Furthermore, it is the only RRAT for which an X-ray counterpart has been discovered (Reynolds et al. 2006; McLaughlin et al. 2007; see also Rea & McLaughlin 2008 for other non-detections). After the serendipitous *Chandra* discovery of its X-ray emission, we performed a 43 ks *XMM-Newton* observation in mid-2006 (McLaughlin et al. 2007). This observation resulted in the detection of strong X-ray pulsations at the radio period, with a $\sim 34\%$ pulsed fraction, and a sinusoidal X-ray pulse profile aligned in phase with the radio bursts. This observation also showed that the spectrum was well modeled by an absorbed blackbody ($N_H = 3.8(2) \times 10^{21} \text{ cm}^{-2}$, $kT = 0.14(1)$ keV, using Anders & Grevesse (1989) solar abundances) and a hint of a power-law component with $\Gamma \sim 2$. Furthermore, a broad spectral absorption line at ~ 1 keV was discovered, and interpreted as either due to resonant cyclotron scattering, to the neutron star atmosphere, or (less likely) to an overabundance of Ne along the line of sight. The unabsorbed flux is $1.5 \times 10^{-13} \text{ erg s}^{-1} \text{ cm}^{-2}$ (0.3–5 keV). This converts to an X-ray luminosity of $L_X \sim 4 \times 10^{33} (d/3.6 \text{ kpc})^2 \text{ erg s}^{-1}$, more than one order of magnitude higher than the spin-down luminosity. Unfortunately, the *XMM-Newton* observation lacked the angular resolution to place meaningful constraints on small-scale extended emission.

We present here the results of a new *Chandra* observation of RRAT J1819–1458. The observation and data reduction are reported in §2, the analysis and results in §3, and a discussion in §4.

2. OBSERVATION AND DATA REDUCTION

The *Chandra* X-ray Observatory observed RRAT J1819–1458 for ~ 30 ks with the Advanced CCD Imaging Spectrometer (ACIS) instrument on 2008 May 31 (ObsID 7645) from 13:33:47 to 22:27:04 (UT) in VERY FAINT (VF) timed exposure imaging mode. We used a 1/8 subarray, which provides a time resolution of 0.4 s, and the typical ACIS-S imaging and spectral information. The source was positioned in the back-illuminated ACIS-S3 CCD at the nominal target position. Standard processing of the data was performed by the *Chandra* X-ray Center to Level 1 and Level 2 (processing software DS 7.6.11.6). The data were reprocessed using the CIAO software (version 4.0). We used the latest ACIS gain map, and applied the time-dependent gain and charge transfer inefficiency corrections. The data were then filtered for bad event grades and only good time intervals were used. No high background events were detected, resulting in a final exposure time of 27.88 ks.

3. ANALYSIS AND RESULTS

3.1. Accurate position

We applied the `wavedetect` tool to the ACIS-S cleaned image, and found two X-ray bright stars in the field detected at a significance of $> 4\sigma$: RRAT J1819–1458 at RA=18:19:34.173 and Dec=–14:58:03.57 (J2000), and another source at RA=18:19:32.36 and Dec=–14:57:58.67 (J2000), with statistical error circles of $0.01''$ and $0.18''$ radii, respectively (see also Fig. 1; all uncertainties in the text are reported at a 1σ confidence level). The latter source is consistent with the 2MASS¹ star 18193233–1457584, which has a position of RA=18:19:32.34, Dec=–14:57:58.5 (with an accuracy of $0.08''$ radius).

We could then perform a bore-site correction of the field to refine the RRAT J1819–1458 position and error circle. There were no problems with the aspect solution during the observation. In particular, the 2MASS position of the source lies within the statistical 1σ uncertainty of the serendipitous X-ray source, and that the next 2MASS source is $8''$ away. Assuming that the association between the 2MASS star and the serendipitous X-ray source is sound, the final RRAT J1819–1458 position is RA=18:19:34.173 and Dec=–14:58:03.57, with a 1σ associated error circle of $0.28''$ radius (derived doing a quadratic mean of all statistical errors plus the 2MASS catalogue intrinsic systematic error). This is the most accurate position for RRAT J1819–1458, reported thus far, more accurate than that achievable through radio timing (Lyne et al. 2009).

3.2. Timing and spectroscopy

For the timing and spectral analysis we extracted the source photons from a circular region with $2.5''$ radius. Circular background regions of radii $2.5''$ and $18''$, far from the source, were used for the timing and spectral analysis, respectively. RRAT J1819–1458 has an ACIS-S 0.3–10 keV count rate of 0.041 ± 0.001 counts/s (background subtracted).

For the timing analysis we corrected the arrival time of each photon to the barycenter of the Solar System (using the JPL-DE405 ephemeris). Using the `Xrons` package, we folded the X-ray data with the radio ephemeris (Lyne et al. 2009), revealing a sinusoidal X-ray modulation with a 0.3–5 keV pulsed fraction of $37 \pm 3\%$, defined as $(F_{\max} - F_{\min}) / (F_{\max} + F_{\min})$, with F_{\max} and F_{\min} the maximum and minimum counts of the X-ray pulse profile.

¹<http://www.ipac.caltech.edu/2mass/>

The source spectrum was rebinned so as to have at least 25 counts per spectral bin. We modeled the spectrum using the XSPEC v.12.1 analysis package. We tried several single component continuum models. The best fit was found with an absorbed blackbody plus an absorption line which we modeled with a Gaussian function. Our best fit values are: $N_H = (6 \pm 2) \times 10^{21} \text{ cm}^{-2}$ and $kT = 0.12 \pm 0.02 \text{ keV}$ for the continuum, and $E_G = 1.0 \pm 0.2 \text{ keV}$, $\sigma_G = 0.12 \pm 0.06 \text{ keV}$, and an equivalent width EQW = $103 \pm 25 \text{ eV}$ for the absorption line ($\chi^2_\nu = 1.02$ (29 dof); see Fig. 2 left panel). The 0.3–5 keV absorbed flux is $F_X = (1.3 \pm 0.2) \times 10^{-13} \text{ erg s}^{-1} \text{ cm}^{-2}$, while the inferred blackbody radius is $2.1 \pm 0.4 \text{ km}$ (assuming a 3.6 kpc distance), smaller than the whole neutron star surface, in accordance with the relatively high pulsed fraction of this X-ray emission.

The pulse profile shape, pulsed fraction, spectral parameters, and flux are all consistent, within the errors, with past measurements (Reynolds et al. 2006; McLaughlin et al. 2007). Therefore, this new *Chandra* observation did not provide any evidence for long term variability. Likewise, no bursts nor aperiodic variations in the X-ray flux were detected over the course of the observation.

Given the paucity of counts we cannot study the spectral line in more detail, and we refer to McLaughlin et al (2007) and Rea et al. (2009 in preparation) for detailed studies based on *XMM-Newton* data. Note that the detection of the $\sim 1 \text{ keV}$ absorption line with *Chandra* shows that the *XMM-Newton* detection was not due to any instrumental effects and confirms the reality of this feature.

3.3. Imaging

The very high-angular resolution of *Chandra* allowed us to perform for the first time an image analysis on angular scales of a few arcseconds (in the previous *Chandra* observation the source was off-axis, affording a limited angular resolution; Reynolds et al. 2006). In Fig. 1 (left) we show the image of the RRAT J1819–1458 field in the 0.3–10 keV energy bands. Extended emission with a complex shape is apparent. There is a more compact emission region extending to radii of roughly $5.5''$, from the pulsar, and then broader diffuse emission extending out to $13''$. In Fig. 1 (right) we show the VLT-NACO K_s field of RRAT J1819–1458 (Rea et al. 2009), which shows that this extended emission cannot be due to the X-ray emission of a cluster of massive stars in the line of sight. To infer the significance and estimate the luminosity of the whole extended emission we built a *Chandra*/*MARX* Point Spread Function (PSF) using the RRAT J1819–1458 spectrum, and subtracted it from the total 0.3–10 keV cleaned image. From the resulting image we extracted all the photons within a $13''$ radius (this roughly corresponds to an extraction from an annular region of

2.5–13'' radii: see Fig. 1 left and Fig. 2 right), and we subtracted from it the background extracted from a similar region far from the source (but in the same S3 CCD). We ended up with an excess of 120 ± 17 counts, which corresponds to a detection significance of $\simeq 7\sigma$. The mean count rate for the whole extended emission within 13'' around the source is then $(4.3 \pm 0.6) \times 10^{-3}$ counts/s in the 0.3–10 keV energy band. Of these counts, 41 ± 9 come from the 5.5'' compact region, with a mean count rate of $(1.5 \pm 0.3) \times 10^{-3}$ counts/s.

In Fig. 2 (right) we compare the background-subtracted surface brightness radial distribution of our *Chandra* observation of RRAT J1819–1458 with that of the *Chandra*/MARX PSF plus a simulated background image. Both surface brightnesses were obtained by extracting counts from 50 annular regions (2 pixels wide each) centered on the source position, and for the RRAT J1819–1458 one, after removal of the serendipitous point source and subtracting the background. This figure shows that extended emission becomes detectable around 5 pixels ($\sim 2.5''$) from the peak of the source PSF. We also performed the same analysis on a Level 2 event file which was re-built turning off the pixel randomization, and applying the background cleaning of the VF mode. This neither changed the results nor improved their significance.

Due to the small number of counts, the spectrum of the diffuse emission is very poorly determined. With 120 counts in the 0.3–10 keV range, we attempted a spectral modelling with a power-law, which gave a good $\chi^2_\nu = 1.07$ (6 dof; see Fig. 2 left; the spectrum was grouped with 15 counts per bin). However, due to the low number of counts the spectral parameters are poorly constrained ($N_H < 7 \times 10^{21} \text{cm}^{-2}$, $\Gamma = 3.0 \pm 1.5$, and a 0.3–5 keV absorbed flux of $(1.6 \pm 0.5) \times 10^{-14} \text{erg s}^{-1} \text{cm}^{-2}$). A blackbody fit was also acceptable ($N_H < 5 \times 10^{21} \text{cm}^{-2}$, $kT = 0.21 \pm 0.12 \text{keV}$), giving a $\chi^2_\nu = 1.04$ (6 dof). However, the blackbody fit showed systematic departures from the data at high energies, and we therefore favor the power-law spectral model. We performed the same fits keeping the N_H fixed at the RRAT J1819–1458 value, finding consistent spectral parameters.

4. DISCUSSION

To date pulsars with observed X-ray nebulae have rotational power \dot{E}_{rot} ranging from $10^{33-39} \text{erg s}^{-1}$ (see Fig. 3), and they are usually rather young ($\tau_c \sim 0.6 - 30 \text{kyr}$). In this respect, interpreting the nebula we see around RRAT J1819–1458 as a spin-down powered PWN is difficult given its low rotational power ($\dot{E}_{\text{rot}} \simeq 3 \times 10^{32} \text{erg s}^{-1}$) and its age ($\tau_c = 117 \text{kyr}$). From the flux of the $\sim 13''$ extended emission (see §3.3), and assuming a 3.6 kpc distance, correcting for absorption and extrapolating the flux in the 0.5–8 keV energy range, we then infer an X-ray efficiency $\eta_X \equiv L_{\text{pwn};0.5-8\text{keV}}/\dot{E}_{\text{rot}} \sim 6 \times 10^{31}/3 \times 10^{32} \simeq 0.2$ for

transferring spin-down power to the X-ray PWN. This X-ray efficiency is relatively high compared to the typical $\eta_X \sim 10^{-6} - 10^{-1}$ observed in other pulsars showing PWNe (see Fig. 3; and also Cheng, Taam & Wang 2004; Gaensler & Slane 2006; Kargaltsev & Pavlov 2008).

One possibility to explain the high X-ray efficiency of this putative PWN might be that the distance is much closer than that inferred from the radio DM of RRAT J1819–1458. If the real distance is e.g. half of the current value (i.e. 1.8 kpc), the X-ray efficiency would be ~ 0.05 , similar to many other pulsars. However, even assuming a smaller distance, the luminosity of this PWN exceeds the upper bound trend for normal pulsars, $\log L_{\text{pwn};0.5-8\text{keV}} = 1.6 \log \dot{E}_{\text{rot}} - 24.2$ (Kargaltsev & Pavlov 2008), which would instead predict a luminosity of $L_{\text{pwn};0.5-8\text{keV}} \sim 5.6 \times 10^{27} \text{ erg s}^{-1}$, very difficult to reconcile with our result, even allowing for a wrong distance for RRAT J1819–1458.

A second possibility might be that the compact $5.5''$ structure we observe is a bow-shock nebula due to the pulsar moving supersonically through the ambient medium. These types of nebulae are indeed more commonly observed in older pulsars. In this scenario, the larger scale extended emission could be part of the remnant of the supernova explosion which formed RRAT J1819–1458. If we interpret the $5.5''$ structure as the termination radius of a bow-shock, we get $R_{\text{TS}} = 2.6 \times 10^{17} \text{ cm}$ (similar to other pulsars; Kargaltsev & Pavlov 2008), from which we infer a projected velocity for RRAT J1819–1458 of $v_p \sim 3 \times 10^{16} \dot{E}_{\text{rot}}^{1/2} n^{-1/2} R_{\text{TS}}^{-1} = 20 \text{ km/s}$, rather small for a pulsar showing a bow-shock considering a reasonable ambient medium density (we assumed here $n=1 \text{ cm}^{-3}$ and a 3.6 kpc distance). On the other hand, if the characteristic age of 117 kyr is correct, we probably would not expect to see a supernova remnant, while assuming a younger age we would not expect a predominantly thermal X-ray emission, with no magnetospheric component as seen for younger pulsars.

A third possibility might be that the nebula around RRAT J1819–1458 gets additional power from the large magnetic energy of this object through mechanisms such as ambipolar diffusion which, instead of going into powering the X-ray emission of this object (as in the magnetar case; Thompson & Duncan 1995), releases its energy in the pulsar wind, or through repeated and powerful transient outbursts (Ibrahim et al. 2004; Halpern et al. 2008; Munro et al. 2007). So far, no magnetically-powered nebula has been detected around magnetars. Many observational biases might have prevented their detection, such as magnetars' large distances, and their very bright emission which usually cannot be observed with high-spatial resolution, but only using 1-dimensional modes (aka timing modes). However, in a very few cases there has been hints for extended emission around magnetars (see e.g. Patel et al. 2003). Beside RRAT J1819–1458 there are seven rotation-powered pulsars with magnetic fields greater than the quantum critical field, and two of them, PSR J1846–0258

and PSR J1119–6127, have PWNe associated (Helfand, Collins & Gotthelf 2003; Gonzalez & Safi-Harb 2003). They have also very high spin-down power ($\dot{E}_{\text{rot}} > 10^{36} \text{erg s}^{-1}$), making difficult any speculation on the possible magnetic contribution to their nebulae. However, note that PSR J1846–0258 did show episodes of magnetar-like activity (Kumar & Safi-Harb 2008; Gavriil et al. 2008), and strong variability has been observed in its PWN (Ng et al. 2009) in coincidence with its outburst, which supports the hypothesis of magnetic energy as an additional energy source to power its PWN. For the remaining five highly magnetic pulsars, it is possible that magnetic-powered nebulae are commonplace, and that selection effects (e.g. the large distances) have precluded us detecting them.

In summary, given the low number of counts we cannot give a conclusive answer on the nature of this extended X-ray emission observed around RRAT J1819–1458. It is clear, however, that with our current picture of PWNe around pulsars, and with the information we now have on RRAT J1819–1458, all traditional interpretations fail at explaining this extended emission. Currently the most viable interpretation seems to be the presence of magnetic contribution to powering of this unusual nebula. Further monitoring observations of RRAT J1819–1458 are crucial to constrain any variability of this extended emission, which could be due to episodic magnetar-like outbursts, as in the case of PSR J1846–0258.

We wish to thank T. Aldcroft and P. Plucinsky for checking the *Chandra* aspect reconstruction during this observation and for useful suggestions, and K. Borkowski, O. Kargaltsev and P. Esposito for comments. NR acknowledges support from an NWO Veni Fellowship. MAM is supported by a WV EPSCoR grant, and a SAO guest investigator grant.

REFERENCES

- Anders, E. & Grevesse, N., 1989, *Geochimica et Cosmochimica Acta* 53, 197
- Arzoumanian, Z., Chernoff, D. F., Cordes, J. M. 2002, *ApJ*, 568, 289
- Cordes, J. M. & Lazio, T. J. W 2002, arXiv:astro-ph/0207156
- Deneva, J. S., et al. 2008, *ApJ* submitted, arXiv:0811.2532
- Gaensler, B. M. & Slane, P. O., 2006, *ARA&A*, 44, 17
- Gavriil, F. P., Gonzalez, M. E., Gotthelf, E. V., Kaspi, V. M., Livingstone, M. A., Woods, P. M 2008, *Science*, 319, 1802
- Gonzalez, M. & Safi-Harb, S. 2003, *ApJ*, 591, L143

- Halpern, J. P., Gotthelf, E. V., Reynolds, J., Ransom, S. M., Camilo, F. 2008, ApJ, 676, 1178
- Helfand, D. J., Collins, B. F., Gotthelf, E. V. 2003, ApJ, 582, 783
- Ibrahim, A. I., et al. 2004, ApJ, 609, L21
- Kargaltsev, O. & Pavlov, G. G, 2008, AIP Conference Proceedings, 983, 171
- Keane, E. F., et al. 2009, MNRAS submitted
- Kennel, C. F. & Coroniti, V. F., 1984, ApJ 283, 694
- Kumar, H. S. & Safi-Harb, S. 2008, ApJ, 678, L43
- Leahy, D. A. & Tian, W. W., 2008, A&A, 480, L25
- Lyne, A., et al. 2009, MNRAS submitted
- McLaughlin M. A., et al. 2006, Nature, 439, 817
- McLaughlin M. A., et al. 2007, ApJ, 670, 1307
- Muno, M. P., Gaensler, B. M., Clark, J. S., de Grijs, R., Pooley, D., Stevens, I. R., Portegies Zwart, S. F., 2008, MNRAS, 378, L44
- Ng, C.-Y., Slane, P. O., Gaensler, B. M., Hughes, J. P. 2009, ApJ, 686,508
- Patel, S. K., et al. 2003, ApJ, 587, 367
- Rea, N. & McLaughlin, M. A. 2008, AIP Conference Proceedings, 968, 151
- Rea, N., et al. 2009, MNRAS submitted
- Reynolds, S. P., et al. 2006, ApJ, 639, L71 Thompson, C. & Duncan, R. C. 1995, MNRAS, 275, 255

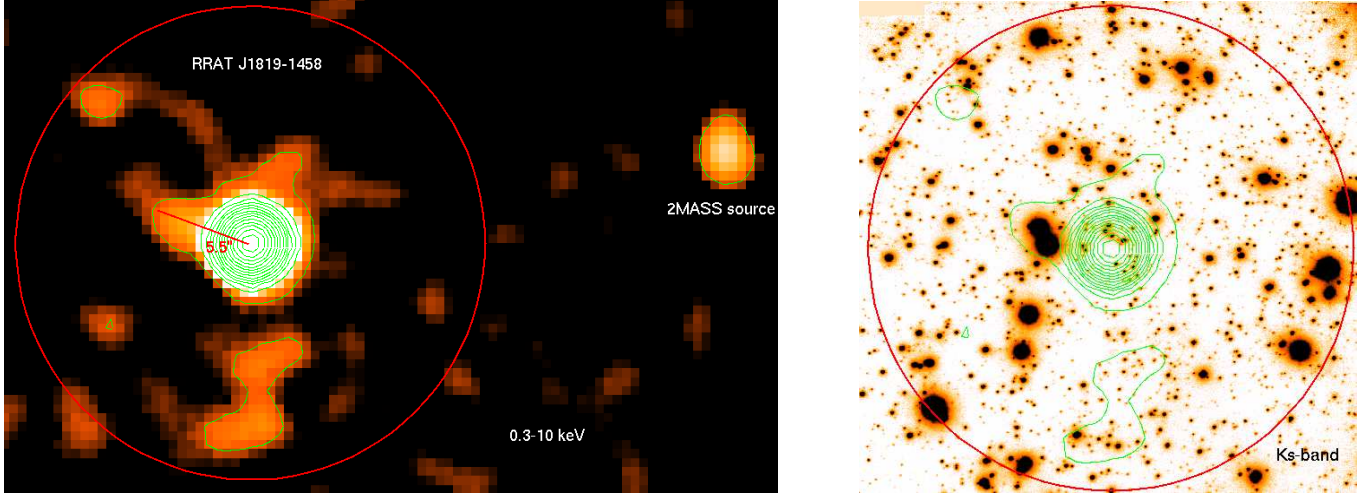


Fig. 1.— *Left Panel:* 0.3–10 keV log-image of our 30 ks *Chandra* ACIS-S observation of RRAT J1819–1458, with a circular region of $13''$ over-plotted, and the contours of the extended emission (from 3σ increasing by 1σ each). The image has been smoothed with a Gaussian function with a radius of 3 pixels. *Right panel:* VLT–NACO image in the K_s -band of the field of RRAT J1819–1458 (Rea et al. 2009) with over-plotted the same circular region and contours as in the left panel. North is top, and East is left.

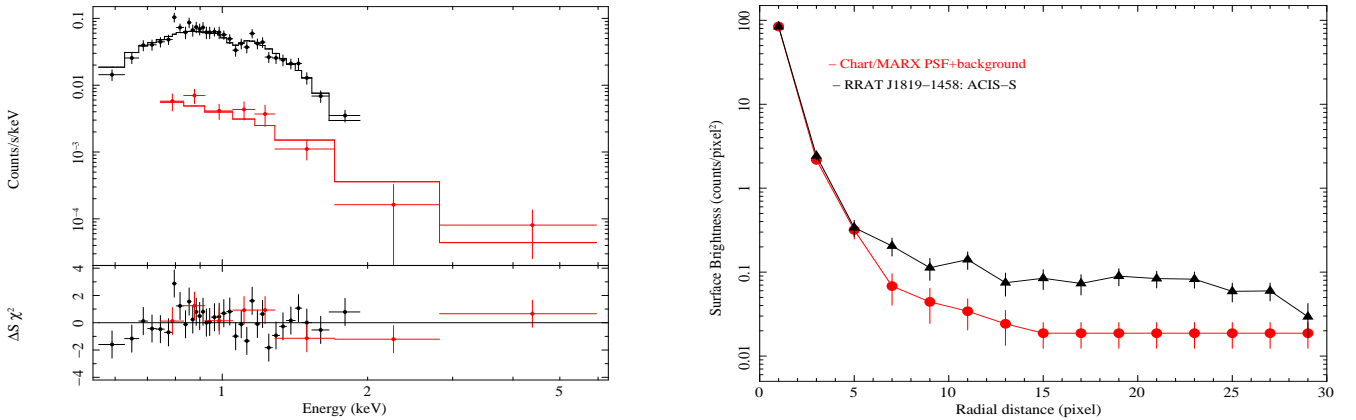


Fig. 2.— *Left panel:* In black we show the ACIS-S spectrum of RRAT J1819–1458 modeled with an absorbed blackbody plus a 1 keV absorption line, while in red we show the spectrum of the extended emission fitted with a power-law. *Right panel:* surface brightness of the background-subtracted ACIS-S image of RRAT J1819–1458 (black) and of the *Chart/MARX* PSF plus a constant background (red). One ACIS-S pixel corresponds to $0.492''$.

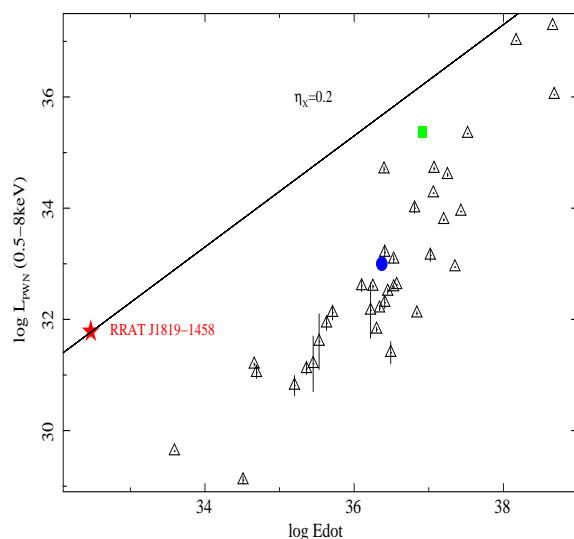


Fig. 3.— Luminosity of all the known X-ray PWNe (in the 0.5–8 keV energy range) compared to the rotational power of the hosted pulsars. All the data, except for RRAT J1819–1458 (this work) and PSR J1846–0258 (revised distance, Leahy & Tian 2008), were taken from Kargaltsev & Pavlov (2008). The green square and blue circle report on the high-B pulsars PSR J1846–0258 and PSR J1119–6127, respectively. The solid line represents $\eta_X = 0.2$. Errors in the pulsar distances are not taken into account in this plot.